*Journal of Sound and Vibration* (1990) **143**(1), 125–142

# EIGENPROBLEM FORMULATION, SOLUTION AND INTERPRETATION FOR NON-PROPORTIONALLY DAMPED CONTINUOUS BEAMS

G. PRATER, JR

*Department of Mechanical Engineering, University of Louisville, Louisville, Kentucky* 40292, *U.S.A.*

AND

R. SINGH

*Department of Mechanical Engineering, The Ohio State University, Columbus, Ohio* 43210, *U.S.A.*

(Received 13 February 1989, and in revised form 17 January 1990)

A rationalized approach is described for formulating the eigenproblems associated with continuous beams where damping non-proportionalities are introduced through the use of lumped dampers, partial damping layers or arbitrary complex impedances. An efficient algorithm is then presented for determining an exact solution to the resulting complex eigenvalue equations, and for computing the coefficients associated with the complex eigenfunctions. A normalization procedure is developed which embodies all pertinent modal information, yet presents the complex modes in a manner which approximates the instantaneous displacement patterns associated with the natural frequencies. This scheme also allows an analyst to assess qualitatively and quantitatively the extent of non-proportionality in the damping distribution and determine which parts of the system it most affects. The formulation and normalization techniques are illustrated with two example cases.

## 1. INTRODUCTION

The partial differential equations of motion governing the free vibration of distributed parameter systems such as strings, rods, shafts and beams can be solved for the classical, undamped case by using standard separation of variables techniques. Such a solution yields real-valued normal modes and natural frequencies. Addition to the mathematical model of viscous damping effects which are uniformly distributed throughout the system also produces a simple solution, but a viscous damping distribution which is not proportional to a linear combination of the inertia and stiffness distributions yields one or more non-linear, complex-valued, transcendental equations which must be simultaneously solved for the eigenvalues.

Distributed parameter solutions are desirable because lumped parameter models, while undoubtedly sufficient for many problems, are still approximations. The discontinuous nature of the generalized co-ordinate system prevents a complete understanding of the system behavior in the presence of non-proportional damping, making it difficult to identify accurately nodal points and higher eigenvalues. A distributed parameter model, on the other hand, has virtually unlimited spatial resolution, which allows physical interpretation of the eigenfunctions and identification of higher eigenvalues.

A disadvantage of the distributed parameter approach, and a reason for its relative lack of use, is that mathematical difficulties make it impossible to apply to systems having



0022-460X/90/220125+18 $03.00/0 

complicated geometries or boundaries. Even so, modal substructuring and synthesis techniques allow distributed parameter models of the simple portions of a system to be used as part of an overall analysis. The more accurate subsystem modal data will then improve results for the entire system.

In this paper eigenproblem formulation, solution and interpretation techniques are presented for non-proportionally damped, transversely vibrating beams. These structures have been chosen as the object of the investigation for several reasons, foremost of which is their wide range of applications. In addition, the partial differential equation of motion for beams is considerably more complicated than the one-dimensional wave equation governing the behavior of other classical continuous systems. Consequently, it is possible to extend the solution and interpretation methodology developed here to non-proportionally damped variations of these systems.

At this point it is necessary to discuss the meaning of the word "proportional" when applied to a damped continuous system. The term is normally applied to discrete systems with Rayleigh damping. Such systems have damping matrices which can be expressed as a linear combination of the mass and stiffness matrices. A more complete definition would specify a discrete system the undamped normal modes of which form the basis of a linear transformation able to simultaneously diagonalize the mass, stiffness and damping matrices. The eigensolution then lies completely within the real domain. Generally, damped systems not meeting these criteria are said to be non-proportionally damped.

Since damping matrices are not part of a distributed parameter analysis, the definition must be modified for the purposes of this study. In the following discussions, the term "non-proportional" will refer to a generally damped system with complex domain modes, one example of which is a continuous system with a damping distribution not proportional to the inertial and stiffness distributions. We will describe the special case of proportional damping where inertia, stiffness and damping effects are all evenly distributed as "uniform damping".

## 2. REVIEW OF PREVIOUS WORK

Begining with the classical paper by Foss [1] on co-ordinate selection and eigenproblem formulation, investigators have studied many aspects of the non-proportional damping problem from a discrete system standpoint; however, the literature on comparable continuous systems is very limited. Al-Jumaily and Faulkner [2] formulated the eigenproblem for continuous beams and circular plates having viscously damped end conditions, but did not solve the resulting frequency equation in the complex domain. Bergman and Nicholson [3] studied continuous beams connected to lumped parameter subsystems (which could include viscous damping), but their approach, based on the Green functions of the subsystems, permitted determination of only undamped modal parameters. Singh and Lyons [4] have shown that it is possible to derive an exact, closed form solution to one-dimensional wave equation problems when non-proportionalities are introduced through the use of a single lumped damper located at a boundary. Zarek and Gibbs [5] performed a similar analysis of Euler beams with lumped impedances at the boundaries, but used a numerical frequency search routine to solve the eigenvalue equation.

In a more recent work Stevens *et al.* [6] discussed the analytical modal analysis of a torsionally vibrating continuous shaft with a partial damping layer. The solution techniques, however, are based in one case on the premise of a small damping assumption, and in another on an energy method involving assumed modes. In a different study, Stevens and Shomstein [7] used energy methods and assumed modes to investigate the behavior of partially damped circular plates. Both the small damping assumption and

assumed modes approach involve approximations which limit their use with heavily non-proportional configurations.

The problems of presenting complex domain modal data has been approached in several ways, all of which have disadvantages. Singh and Lyons presented the modes as complex domain plots. These plots, which have also been used to display the modes of non-proportionally damped discrete systems [8], are difficult to interpret because there is no explicit spatial scale. Zarek and Gibbs displayed the data as a sequence of instantaneous modal displacement plots equally spaced over a half-cycle of motion. This approach has limitations in that it does not accurately identify points of minimum displacement magnitude, and because it does not present the actual complex modes. In addition, the method bears little resemblance to real domain normalization techniques, and yields results which are difficult to physically interpret. The authors of references [6] and [7] presented the eigenfunctions as simple magnitude plots, with no reference to the phase angles.

To summarize, one can say that mathematical difficulties have limited the study of generally damped continuous system. The available literature tends either to introduce approximations as part of the problem solution technique, thus eliminating part of the appeal of a distributed parameter solution, or else concentrate on simple system configurations with lumped damping at boundary locations. There are also no studies which explicitly address the normalization problem or attempt to quantify the extent of non-proportionality in the damping distribution.

## 3. EIGENPROBLEM FORMULATION

Consider a transversely vibrating beam subjected to an arbitrary number of lumped viscous dampers and partial viscous damping layers (see Figure 1). If one defines segment boundaries at lumped damper locations and at the beginning and end of distributed layers, the equation of motion for those segments subjected to only lumped damping can be written in non-dimensional form as

$$\partial^4 y/\partial x^4 + \alpha^4 \partial^2 y/\partial t^2 = 0, \tag{1}$$

where $y$ is the transverse displacement, $x$ is the axial spatial co-ordinate, and $\alpha$ is a real constant. Variables $y$, $x$, $\alpha$ and $t$ are related to dimensional quantities as follows:

$$y = \bar{y}/L, \qquad t = \bar{t}/\tau, \qquad x = \bar{x}/L, \qquad \alpha^4 = (L^4\rho)/(\tau^2 EIg_c). \tag{2c, d}$$

Here $L$ is the beam length, $g_c$ is the gravitational constant, and $\tau$ is an arbitrary time constant chosen as one second. For a segment covered with a uniform viscous damping layer, the equation of motion becomes

$$\partial^4 y/\partial x^4 + c_d\, \partial y/\partial t + \alpha^4 \partial^2 y/\partial t^2 = 0, \tag{3}$$

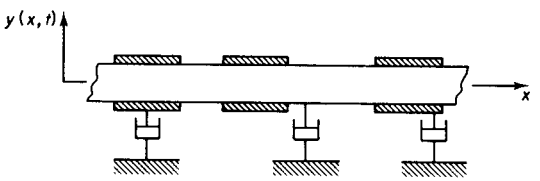


Figure 1. Transversely vibrating beam with arbitrarily spaced and sized lumped or distributed viscous damping layers. The beams may have either classical boundary conditions, or damping/stiffness/inertia elements at the boundaries.

where the dimensionless distributed damping coefficient $c_d$ is given by

$$c_d = \bar{c}_d L^4/\tau EI. \tag{4}$$

If one denotes the beginning of a segment by 1, the end by 2, and assumes the partial differential equations of motion to be separable, the solution to equations (1) and (3) can be written as

$$y(x, t) = \Phi_{ni}(x)\, e^{\gamma_n t} \qquad (x_{i1} \leqslant x \leqslant x_{i2}). \tag{5}$$

Here $\Phi_{ni}$ is the $n$th eigenfunction for the $i$th beam segment. Note that each eigenfunction is valid for only those axial locations which lie within its corresponding segment.

While one would expect the spatial part of the solution to change with respect to the axial location, the time dependent part should be the same for all segments, and this is indeed the case. The constant $\gamma$ is the $n$th complex natural frequency, and can be written as

$$\gamma_n = -\zeta_n\omega_n \pm i\omega_n\sqrt{(1-\zeta_n^2)}, \tag{6}$$

where $\zeta$ and $\omega$ are the $n$th damping ratio and undamped natural frequency, respectively, and $i = \sqrt{-1}$.

Inserting equation (5) into equation (1), simplifying the result, and dropping the modal index yields the following ordinary differential equation for an undamped segment:

$$d^4\Phi_i/dx^4 + \beta^4\Phi_i(x) = 0. \tag{7}$$

The complex eigenvalue, $\beta$, is defined in terms of the beam natural frequencies and physical properties as

$$\beta_n^4 = \alpha^4\gamma_n^2. \tag{8}$$

The general solution to equation (7) now becomes

$$\Phi_i(x) = B_{i1}\cosh\beta x + B_{i2}\sinh\beta x + B_{i3}\cos Bx + B_{i4}\sin\beta x, \tag{9}$$

where $B_1$, $B_2$, $B_3$ and $B_4$ are complex constants.

For viscously layered segments, the eigenvalue equation and eigenfunctions will be identical to those of an undamped beam segment having similar constraint conditions. While equations (7) and (9) are still valid, the eigenvalues are different, and can be expressed in terms of the complex natural frequencies as

$$\beta_n^4 = \alpha^4\gamma_n^2 + c_d\gamma_n. \tag{10}$$

Solution of the eigenproblem involves determination of the complex natural frequencies and eigenfunction coefficients. This can be accomplished by applying boundary conditions to equation (9), and imposing shear, moment and continuity constraints to the segment interfaces. The boundary conditions may be classical, in which case two of the following will be valid:

$$\Phi(x=b)=0, \qquad d\Phi(x=b)/dx=0, \qquad d^2\Phi(x=b)/dx^2=0, \qquad d^3\Phi(x=b)/dx^3=0. \tag{11a-d}$$

If a lumped damper is present at the boundary, (11d) becomes

$$d^3\Phi(x=b)/dx^3 = -c_1\gamma\Phi(x=b), \qquad c_1 = \bar{c}_1 L^3/\tau EI. \tag{12a, b}$$

Note that equation (12a) can easily be modified to accommodate more complicated lumped mechanical impedances. At the interface between segments $i$ and $j$, the constraint conditions are

$$\Phi_i(x_{i2}) = \Phi_j(x_{j1}), \qquad d\Phi_i(x_{i2})/dx = d\Phi_j(x_{j1})/dx, \tag{13a, b}$$

$$d^2\Phi_i(x_{i2})/d^2x = d^2\Phi_j(x_{j1})/d^2x, \qquad d^3\Phi_i(x_{i2})/d^3x = d^3\Phi_j(x_{j1})/d^3x. \tag{13c, d}$$

If a lumped damper is present at the interface, the shear force balance of condition (13d) becomes

$$d^3\Phi_i(x_{i2})/d^3x + c_1\gamma\Phi_i(x_{i2}) = d^3\Phi_j(x_{j1})/d^3x. \tag{14}$$

The lumped and distributed dampers of equations (3), (10), (12) and (14) can, if necessary, be replaced with mechanical impedance elements such that

$$z_1(\gamma) = \bar{z}_1 L^3/\tau EI, \qquad z_d(\gamma) = \bar{z}_d L^2/EA\tau. \tag{15}$$

One can now complete the eigenproblem formulation by expressing the boundary and segment interface conditions in matrix form as

$$[\Psi]\{B\} = \{0\}, \tag{16}$$

where $[\Psi]$ is a $4m \times 4m$ constraint matrix, the functional elements of which depend on $\gamma$ only, $\{B\}$ is a $4m$ column vector containing the unknown eigenfunction coefficients, and $\{0\}$ is a $4m$ null vector.

## 4. EIGENPROBLEM SOLUTION

The degree of coupling between the eigenfunction coefficients, the inherent non-linearity of the boundary and constraint condition equations, and the fact that the solution to equation (16) lies within the complex domain all mean that a numerical technique must be used to determine $\gamma$ and $\{B\}$. That proposed here involves the following steps.

1. An initial guess for $\gamma$ is substituted into constraint equation (16).
2. A series of linear transformations is used to manipulate the constraint matrix $[\Psi]$ into upper triangular form. The final element in the last row (denoted by $\delta$) then represents a residual functional value for the complex frequency equation.
3. A convergence test is applied. If $\delta$ lies within a desired tolerance about the point (0·0, 0·0), the current $\gamma$ value is assumed to be a solution. Back substitution is then used to determine the eigenfunction coefficients.
4. If convergence is not achieved, $\delta$ and its derivative with respect to $\gamma$ are used in conjunction with a modified Newton's method to compute a new frequency guess. Steps (2) and (3) are then repeated.

After $\gamma$ and $\{B\}$ have been determined, modal parameters can be computed by using equation (6), and the eigenfunctions can be constructed by substituting the appropriate coefficient values into equation (9).

### 4.1. DETERMINATION OF FUNCTIONAL VALUES

It has been found that the solution algorithm is relatively insensitive to the initial frequency guess. However, selection of values which are too far from the actual root may result in convergence to an undesired eigenvalue. In general, starting values of $\gamma_n = (\varepsilon + i\omega_n)$, where $\varepsilon$ is a small negative number, give good results for moderately damped systems. For heavily damped configurations, one can assure convergence by using the solution algorithm to determine precisely the eigenvalues for a lightly damped case. Damping is then added, and the entire procedure is repeated using the eigenvalues from the previous trial as a starting point. Continuing in this manner allows one to find solutions for very heavily damped systems, and at the same time shows the effects of incrementally increased damping.

Determination of functional values for the eigenvalue equation is considerably more difficult. The triangularization procedure of step (2) must occur in the complex domain while introducing little error into the computations. It can be efficiently implemented by

using Gaussian elimination with partial pivoting. The last row in $[\Psi]$ then represents an equation of the form

$$\psi_{nn}B_n = F(\gamma)B_n = \delta, \tag{17}$$

where $F(\gamma)$ is a functional value for the frequency equation. Since the choice of a single non-zero eigenfunction coefficient is arbitrary, one can choose

$$B_n = (1{\cdot}0, 0{\cdot}0). \tag{18}$$

The functional value then becomes

$$F(\gamma) = \delta. \tag{19}$$

### 4.2. CONVERGENCE TEST

Because the augmentation column in a standard Gaussian elimination procedure is in this case a null vector which is unaffected by the triangularization procedure, $\delta$ must approach zero for $\gamma$ to be a valid eigenvalue. One can now specify a convergence criterion as

$$\mathrm{Re}\,(\delta) < \varepsilon_r, \qquad \mathrm{Im}\,(\delta) < \varepsilon_i, \tag{20a, b}$$

where $\varepsilon_r$ and $\varepsilon_i$ are small numbers representing the real and imaginary parts of the criterion, respectively.

### 4.3. COEFFICIENT DETERMINATION

If equation (20) is satisfied, $\gamma$ can be assumed to be a solution and used to determine the eigenfunction coefficients. Back substitution into the triangular constraint matrix gives these as

$$B_j = \sum_{i=j}^{n} B_i\psi_{ij}, \qquad j = n-1, n-2, \ldots, 1. \tag{21}$$

### 4.4. EIGENVALUE CORRECTION

If the convergence criterion is not satisfied, a new frequency guess must be calculated. To do so, one can note that for a complex-valued equation $F(\gamma)$ to be satisfied, both its real and imaginary components must be identically zero. In mathematical terms

$$\mathrm{Re}\,(F(\gamma)) = f(u, v) = 0, \qquad \mathrm{Im}\,(F(\gamma)) = g(u, v) = 0, \tag{22a, b}$$

where $u$ and $v$ are the real and imaginary parts of $\gamma$, respectively. These relations represent a system of two coupled, non-linear equations in $u$ and $v$. Given an initial guess for $\gamma$, corrected values can be computed by using the formulas

$$u_n = u_m + h_m, \qquad v_n = v_m + k_m, \tag{23a, b}$$

where $h$ and $k$ satisfy

$$\frac{\partial f(u_m, v_m)}{\partial u}(h_m) + \frac{\partial f(u_m, v_m)}{\partial v}(k_m) = -f(u_m, v_m), \tag{24a}$$

$$\frac{\partial g(u_m, v_m)}{\partial u}(h_m) + \frac{\partial g(u_m, v_m)}{\partial v}(k_m) = -g(u_m, v_m), \tag{24b}$$

and $m = n-1$. The partial derivatives of $f(u, v)$ and $g(u, v)$ can be computed by using the Cauchy-Riemann equations:

$$\frac{\mathrm{d}F(\gamma)}{\mathrm{d}\gamma} = \frac{\partial f(u, v)}{\partial u} + \mathrm{i}\frac{\partial g(u, v)}{\partial u}, \qquad \frac{\mathrm{d}F(\gamma)}{\mathrm{d}\gamma} = \frac{\partial g(u, v)}{\partial v} - \mathrm{i}\frac{\partial f(u, v)}{\partial v}. \tag{25a, b}$$

The derivative of the functional value is determined in the following manner. A derivative constraint matrix $[\Psi]'$ is generated by performing an element-by-element differentiation of the original constraint matrix. Mathematically,

$$\psi'_{ij} = \mathrm{d}\psi_{ij}/\mathrm{d}\gamma. \tag{26}$$

While $[\Psi]$ is being triangularized, the chain rule is used to keep its derivative matrix current. As an example, consider the sequence of operations used to create zeros in the second through $n$th row. If one denotes the original elements by the subscript $o$, and the transformed elements by $t$, one has

$$\psi_{ij,t} = \psi_{ij,o} - \psi_{i1,o}\psi_{ij,o}/\psi_{11,o}. \tag{27}$$

The operations required to compute the new $i$th row of the constraint derivative matrix are

$$\psi'_{ij,t} = \psi'_{ij,o} - \frac{\psi'_{i1,o}\psi_{1j,o}}{\psi_{11,o}} - \frac{\psi_{i1,o}\psi'_{1j,o}}{\psi_{11,o}} + \frac{\psi_{i1,o}\psi_{1j,o}\psi'_{11,o}}{\psi^2_{11,o}}. \tag{28}$$

Similar operations are performed for the second through $n-1$ columns. When these are completed, the required constraint derivative is given by

$$\mathrm{d}F(\gamma)/\mathrm{d}\gamma = \psi'_{nn}. \tag{29}$$

A corrected eigenvalue can now be computed. The results of equation (24) are substituted into equation (23) to yield the new complex natural frequency. This value is then substituted into the original constraint equation, and steps (2)-(4) of the solution algorithm are executed. The entire process is repeated until equation (20) is satisfied.

## 5. EIGENFUNCTION NORMALIZATION

At this point the question of normalization arises. An obvious possibility is to divide each complex eigenfunction $\Phi(x)$ by the magnitude of its largest displacement, $\Phi(x_m)$, giving

$$\tilde{\Phi}(x) = \Phi(x)/|\Phi(x_m)|. \tag{30}$$

The result can then be displayed as either magnitude and phase versus $x$, or real part and imaginary part versus $x$. This approach has the appeal of simplicity and similarity to real-valued techniques but, as will be seen in the example cases, problems of interpretation arise.

We now present a more refined scheme. Magnitudes are defined as

$$|\tilde{\Phi}(x)| = \sigma(x)|\tilde{\phi}(x)|, \tag{31}$$

where

$$\tilde{\phi}(x) = \Phi(x)|\Phi(x_b)|/\Phi(x_b)|\Phi(x_m)|. \tag{32}$$

Here $x_b$ is the axial location of the damping element having the largest effect on the system response, and $\Phi(x_m)$ is the modal displacement with the largest magnitude. The quantity $\sigma(x)$ in equation (31) is a unit sign function, the value of which is set equal to $+1$ at $x = x_m$, and then changes sense every time the magnitude of $\Phi(x)$ passes through a relative minimum. The normalized phases are defined as

$$\theta(x) = \tan^{-1}[\mathrm{Im}(\tilde{\phi}(x))/\mathrm{Re}(\tilde{\phi}(x))] - (\pi/2)[1-\sigma(x)], \tag{33}$$

where the branch cut in the complex plane is assumed to lie along the negative real axis. Similarly, the normalized real and imaginary parts of the eigenfunctions are given by

$$\tilde{\Phi}_r(x) = \mathrm{Re}\,[\tilde{\phi}(x)] \qquad \text{and} \qquad \tilde{\Phi}_i(x) = \mathrm{Im}\,[\tilde{\phi}(x)]. \tag{34}$$

Note that the factor of $\pi/2$ in equation (33) accounts for the sign changes induced by $\sigma(x)$, and assures that the combination of the normalized magnitude and phase represents the same complex number as is given by equation (30).

## 6. EXAMPLE CASES

The formulation, solution and normalization algorithms of sections 3–5 have been implemented in a FORTRAN computer program. To illustrate their use, we consider the systems of Figure 2. Figure 2(a) represents a uniform beam with a simple support at $x = 0$ and a lumped damper at $x = 1{\cdot}0$, while in Figure 2(b) is depicted a beam which has simple supports at $x = 0$ and $x = 1{\cdot}0$, a section change at $x = x_d$, and a distributed damping layer extending from $x = 0$ to $x = 1{\cdot}0$. Double precision variables were used in all critical computations, and a convergence criterion of $1{\cdot}0 \times 10^{-8}$ was specified for equation (19). Functional values for the complex modes were computed and plotted at 100 equally spaced points.

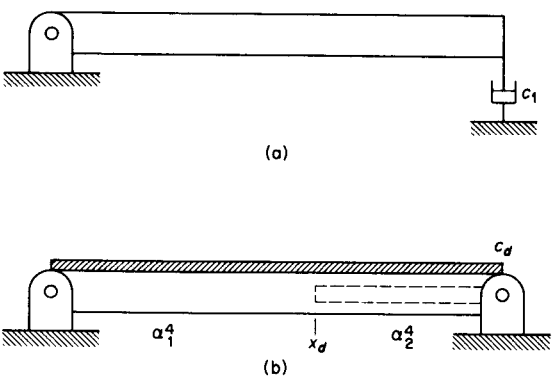


Figure 2. (a) Example case 1 and (b) example case 2 beam configurations.

### 6.1. EXAMPLE CASE 1

The system of Figure 2(a), with its single lumped damper located at a boundary, is representative of the simplest possible damping configuration. The origin of the non-proportionalities is obvious, since the damping effect is localized and the inertia and stiffness effects are uniformly distributed. A configuration of this type might arise in an effort to model foundation interaction in earthquake-excited buildings or energy dissipation mechanisms in the joints of space structures.

#### 6.1.1. *Eigenproblem formulation*

The beam has one segment, and boundary conditions of

$$\Phi(0) = 0, \qquad \mathrm{d}^2\Phi(0)/\mathrm{d}^2x = 0, \tag{35a, b}$$

$$\mathrm{d}^2\Phi(1)/\mathrm{d}^2x = 0, \qquad \mathrm{d}^3\Phi(1)/\mathrm{d}^3x + c_1(\beta^2/\alpha^2)\Phi(1) = 0. \tag{35c, d}$$

When expressed in the form of constraint equation (23), these become

$$\begin{bmatrix} 1{\cdot}0 & 0{\cdot}0 & 1{\cdot}0 & 0{\cdot}0 \\ 1{\cdot}0 & 0{\cdot}0 & -1{\cdot}0 & 0{\cdot}0 \\ \cosh(\beta) & \sinh(\beta) & -\cos(\beta) & -\sin(\beta) \\ (\alpha^2\beta)\sinh(\beta) & (\alpha^2\beta)\cosh(\beta) & (\alpha^2\beta)\sin(\beta) & -(\alpha^2\beta)\cos(\beta) \\ +c_1\cosh(\beta) & +c_1\sinh(\beta) & +c_1\cos(\beta) & +c_1\sin(\beta) \end{bmatrix} \begin{Bmatrix} B_1 \\ B_2 \\ B_3 \\ B_4 \end{Bmatrix} = \begin{Bmatrix} 0 \\ 0 \\ 0 \\ 0 \end{Bmatrix}. \quad (36)$$

Manual application of equations (35a) and (35b) shows that $B_1 = B_3 = 0$, which reduces equation (36) to

$$\begin{bmatrix} \sinh(\beta) & -\sin(\beta) \\ (\alpha^2\beta)\cosh(\beta) + c_1\sinh(\beta) & -\alpha^2\beta\cos(\beta) + c_1\sin(\beta) \end{bmatrix} \begin{Bmatrix} B_2 \\ B_4 \end{Bmatrix} = \begin{Bmatrix} 0 \\ 0 \end{Bmatrix}. \quad (37)$$

The derivative of the constraint matrix is then

$$[\Psi]' = \frac{1}{2\alpha\sqrt{\gamma}} \begin{bmatrix} \cosh(\beta) & -\cos(\beta) \\ \alpha^2\cosh(\beta) + (c_1 + \alpha^2\beta)\sinh(\beta) & \alpha^2\cos(\beta) + (c_1 + \alpha^2\beta)\sin(\beta) \end{bmatrix}. \quad (38)$$

The constant $\alpha^4$ was specified as 3·0, and non-proportionality was introduced by increasing $c_1$ from 0·0 in increments of 0·9. Initial guesses for the solution algorithm were determined by inspection of the classical undamped frequency equation. This has roots at zero, corresponding to a rigid-body mode, and at

$$\beta = [(4n-3)\pi/4] - \varepsilon, \qquad n = 1, 2, \ldots, \quad (39)$$

where $\varepsilon$ is a small real constant.

### 6.1.2. *Results and discussion*

Graphical results for this case are shown in Figures 3–13. The solution algorithm yields the appropriate classical eigenvalues and eigenfunctions for the undamped case. The real parts of the computed eigenvalues are of the order of $1{\cdot}0 \times 10^{-14}$ (compared with the exact value of 0·0), while the imaginary parts are identical to published values. Inspection of the modes (see Figure 3) shows that the complex modulus appears as a signed magnitude, that there are well defined nodal points and that the phase angles are identically zero.

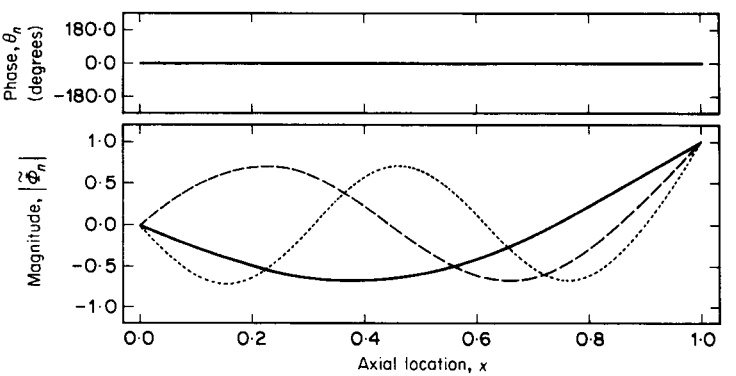


Figure 3. Normalized magnitude and phase for example case 1 eigenfunctions, $c_1 = 0{\cdot}0$. ——, Mode 1 ($\gamma_1 = 0{\cdot}000 \pm 8{\cdot}902$i); – – –, mode 2 ($\gamma_2 = 0{\cdot}000 \pm 28{\cdot}85$i); · · · ·, mode 3 ($\gamma_3 = 0{\cdot}000 \pm 60{\cdot}19$i).

Thus far the analysis agrees with results from classical beam theory; however, for a $c_1$ value of 2·7, several changes in the eigenfunctions are apparent (see Figure 4). Although the general shapes of magnitude curves are similar to those of the undamped case, there are no points of zero displacement except where specified by the boundary condition at $x = 0$. This behavior means that in the traditional definition of the term, there are no nodes on a non-proportionally damped structure. Instead, there are points where the modal displacement is locally minimized, and points where the displacement is instantaneously zero. These locations do not generally coincide, nor are the instantaneous zeros fixed. Near what were once nodal points, there are pronounced discontinuities in the eigenfunction curves. It should be noted that these discontinuities are a result of the normalization scheme; when magnitude and phase plots are considered together, they represent functions which are continuous in the complex plane. It is also shown in Figure 4 that the phases are no longer identically zero, and that the deviations are also largest near the undamped nodes. The normalized modes for $c_1 = 7{\cdot}2$ (see Figure 5) show similar trends, but indications of non-proportionality are much more pronounced.

Instantaneous modal displacements represent the actual shape of the beam as it vibrates at a natural frequency, and provide a physical interpretation for the normalized eigenfunction plots. In Figure 6 ($c_1 = 7{\cdot}2$) are shown the beam displacements at seven equal time intervals over one half-cycle. One can see that the non-zero phases result in motion which no longer has the synchronous quality characteristic of real domain modes. Deviations

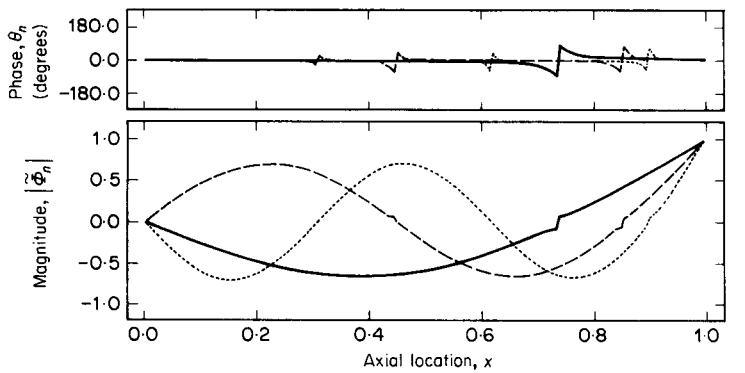


Figure 4. Normalized magnitude and phase for example case 1 eigenfunctions, $c_1 = 0{\cdot}09$. ——, Mode 1 ($\gamma_1 = -0{\cdot}5975 \pm 8{\cdot}832i$); - - -, mode 2 ($\gamma_2 = -0{\cdot}5987 \pm 28{\cdot}81i$); · · · ·, mode 3 ($\gamma_3 = -0{\cdot}5992 \pm 60{\cdot}16i$).

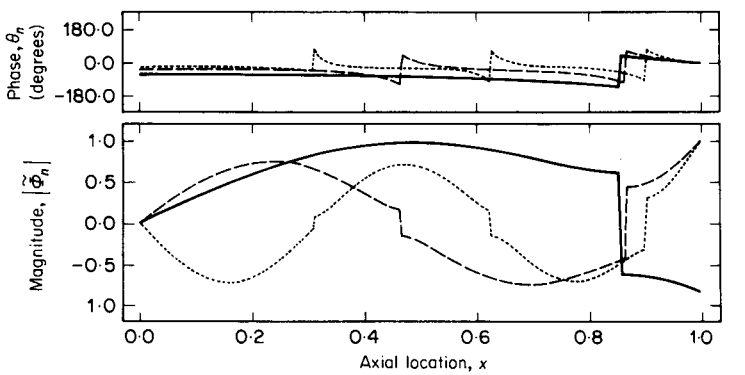


Figure 5. Normalized magnitude and phase for example case 1 eigenfunctions, $c_1 = 7{\cdot}2$. ——, Mode 1 ($\gamma_1 = -1{\cdot}435 \pm 6{\cdot}054i$); - - -, mode 2 ($\gamma_2 = -3{\cdot}655 \pm 26{\cdot}20i$); · · · ·, mode 3 ($\gamma_3 = -4{\cdot}303 \pm 58{\cdot}29i$).

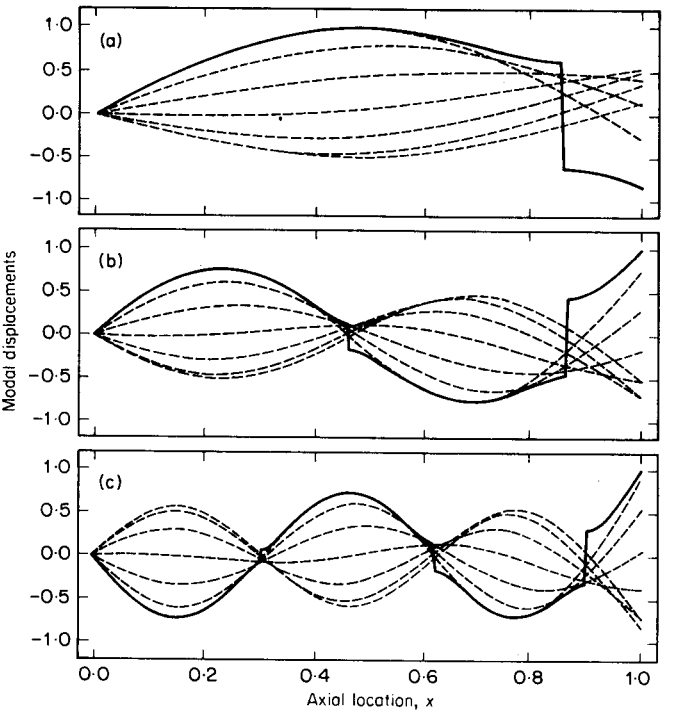


Figure 6. Time dependent modal displacements associated with example case 1 complex eigenfunctions, $c_1 = 7{\cdot}2$. (a) Mode 1, (b) Mode 2, (c) Mode 3. ——, Normalized magnitude; - - - -, instantaneous modal displacement.

from classical behavior are most pronounced near the largest-magnitude discontinuity and, in fact, the normalized magnitude can be thought of as an envelope within which the displacements occur.

In Figures 7–9 we illustrate the utility of our normalization scheme by displaying the modal data of Figures 5 and 6 using alternative presentation techniques. Simple, non-signed magnitudes and phases of the type used by Stevens *et al.* in reference [6] are depicted in Figure 7. The effect is such that plotted magnitudes do not match the characteristic shape assumed by the beam when it is vibrating at a natural frequency,

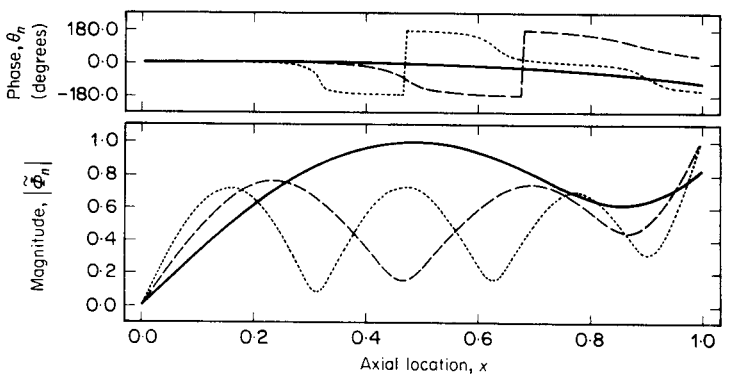


Figure 7. Partially normalized magnitude and phase for example case 1 eigenfunctions, $c_1 = 7{\cdot}2$. ——, Mode 1; - - -, mode 2; · · · ·, mode 3.

which makes physical interpretation difficult. In addition, the phase angles now deviate from ±180 degrees as well as zero. Note that although Figures 5 and 7 look quite different, they display exactly the same complex numbers.

When the data is presented as separate real and imaginary plots (see Figure 8), one again has interpretation problems. The method does have an advantage in that comparison of the relative amplitude of the component functions allows assessment of the extent of the non-proportionality, a fact which will shortly be used to define formally a numerical index. One also sees that the real parts of the complex eigenfunctions assume the shapes of classical undamped modes, while the imaginary parts assume the shapes associated with an infinitely damped beam (simply supported at both ends). This behavior is characteristic of simple lumped damping configurations, but not of more complicated cases. Finally, complex domain plots (see Figure 9) as used in references [4] and [8] present the greatest interpretation difficulties; the functions do not resemble the modal displacements, nor is there an explicit spatial scale.

A plot of the natural frequencies in the complex plane (see Figure 10) provides insight into the behavior of the system under incrementally increased non-proportional damping. The undamped values for all three modes exhibit identically zero real parts, and for each there exists a damping level for which this real part is maximized. Further increases result in a reduced energy dissipation effect. In the limit as $c_1$ approaches infinity, the real part approaches zero, and the imaginary part approaches the value of the undamped natural

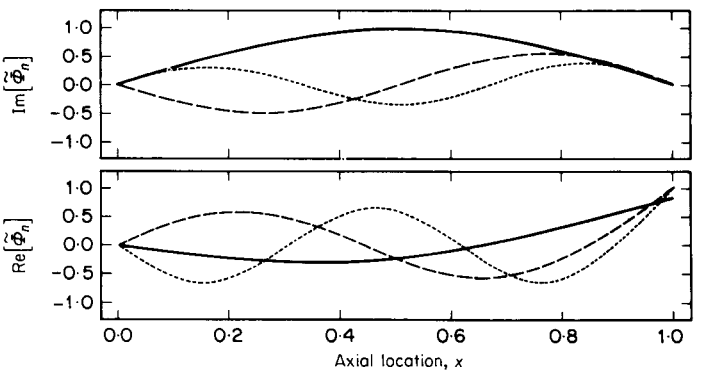


Figure 8. Real and imaginary parts of example case 1 eigenfunctions, $c_1 = 7{\cdot}2$. ——, Mode 1; - - -, mode 2; · · · ·, mode 3.

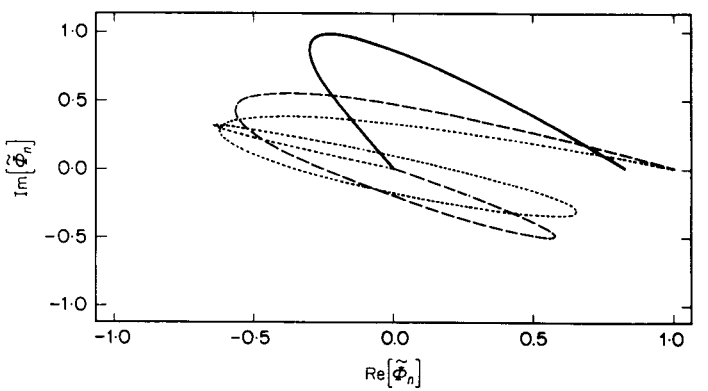


Figure 9. Imaginary part versus real part of example case 1 eigenfunctions, $c_1 = 7{\cdot}2$. ——, Mode 1; - - -, mode 2; · · · ·, mode 3.

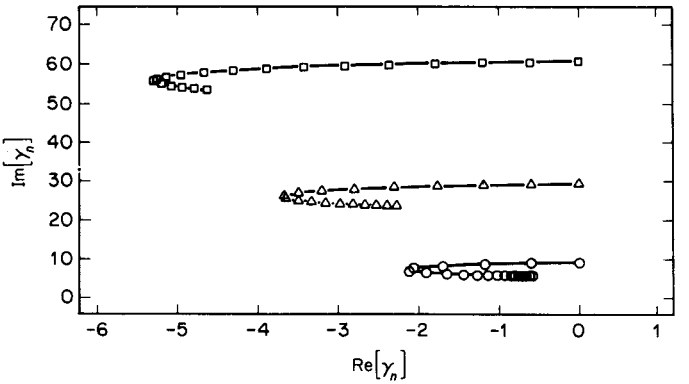


Figure 10. Variation of example case 1 complex natural frequencies with increasing damping coefficient. ○—○, Mode 1; △—△, mode 2; □—□, mode 3.

frequency for a beam with a simply supported boundary at the damper location. Plots of the system damping ratios (see Figure 11) also reflect these trends.

In Figures 12 and 13 are shown the effect of damping on maximum Im/Re ratios and magnitude discontinuities of the eigenfunctions. Here the maximum Im/Re ratio is defined

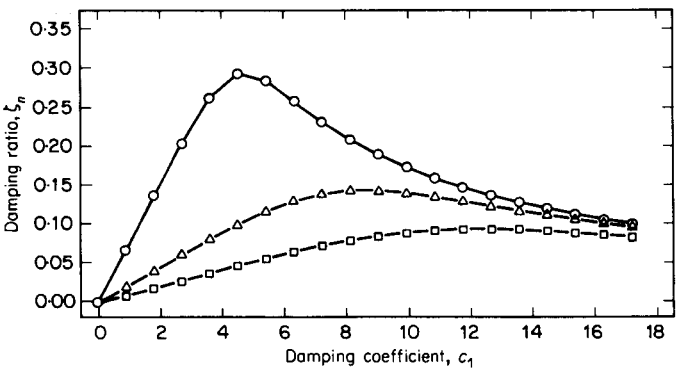


Figure 11. Damping ratio versus non-dimensional damping coefficient, example case 1. ○—○, Mode 1; △—△, mode 2; □—□, mode 3.

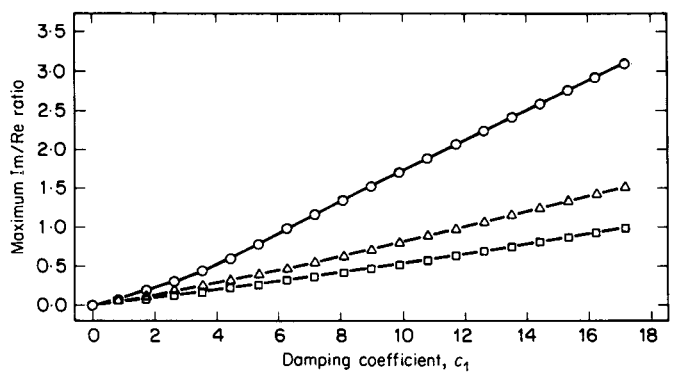


Figure 12. Maximum magnitude discontinuity versus non-dimensional damping coefficient, example case 1. ○—○, Mode 1; △—△, mode 2; □—□, mode 3.

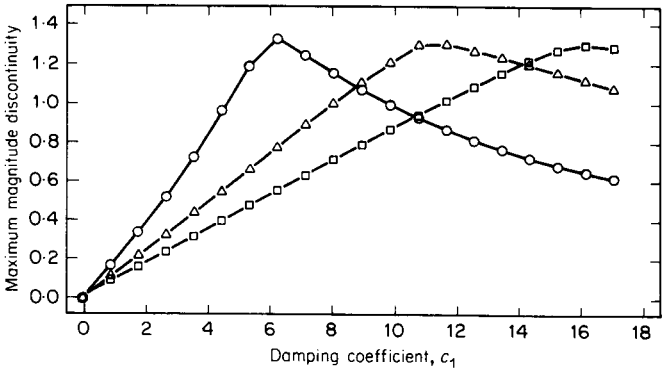


Figure 13. Maximum imaginary/real ratio of eigenfunctions versus non-dimensional damping coefficient, example case 1. ○—○, Mode 1; △—△, mode 2; □—□, mode 3.

as

$$(\mathrm{Im}/\mathrm{Re})_n = |\max\{\mathrm{Im}(\Phi_n(x))\}/\max\{\mathrm{Re}(\Phi_n(x))\}|. \tag{40}$$

Given the form of our normalization procedure, this ratio will be very small or very large for near-proportional damping configurations, and close to 1·0 for heavily non-proportional configurations. Therefore, one can use the Figure 12 results to define a non-proportionality index as

$$\delta_{n1} = (\mathrm{Im}/\mathrm{Re})_n \qquad (0{\cdot}0 < \mathrm{Im}/\mathrm{Re} < 1{\cdot}0), \tag{41a}$$

or

$$\delta_{n1} = 1/(\mathrm{Im}/\mathrm{Re})_n \qquad (\mathrm{Im}/\mathrm{Re} > 1{\cdot}0). \tag{41b}$$

With this definition, $\delta_{n1}$ will range between zero, representing an undamped or proportionally damped system, and unity, representing the highly non-proportional case in which the real and imaginary components of the eigenfunction are equal in magnitude. The following criterion must be satisfied for a proportional damping approximation to be valid:

$$\delta_{n1} \ll 1{\cdot}0. \tag{42}$$

The maximum magnitude discontinuities of Figure 13 also denote non-proportionality, and already exhibit the increasing/decreasing form embodied in equation (41). Since the discontinuity is twice the modal magnitude, an index can be defined as

$$\delta_{n2} = \max|\Phi_n(x = x_m)|, \tag{43}$$

where $x_m$ is the location of the discontinuity. Again, $\delta_{n2}$ will range between 0 and 1, and the proportional damping criterion is

$$\delta_{n2} \ll 1{\cdot}0. \tag{44}$$

Both indices show that maximum non-proportionality occurs in this case at approximately $c_1 = 6{\cdot}0$ for mode 1, $c_1 = 11{\cdot}0$ for mode 2 and $c_1 = 17{\cdot}0$ for mode 3.

### 6.2. EXAMPLE CASE 2

The beam of Figure 2(b) is an example of a system having a distributed viscous damping layer, but on the basis of a cursory examination it appears to be proportionally damped. The damping layer uniformly covers the entire surface, and there are no lumped inertia,

stiffness or damping elements. There is, however, an abrupt inertia/stiffness change at $x = x_d$ corresponding to an instantaneous change in the constant $\alpha^4$. The fact that the damping effect is uniformly distributed while the stiffness and inertia properties are not means that although the damping distribution is uniform, it is still non-proportional. Physically, such a configuration could arise when a partially hollow beam is subjected to a viscous damping effect, or when two beams of different cross-section are butt welded together.

6.2.1. *Problem formulation*

There are two beam segments, and upon dropping the modal index, the constraint conditions can be written as

$$\Phi_1(0) = 0, \qquad d^2\Phi_1(0)/dx^2 = 0, \tag{45a, b}$$

$$\Phi_1(x_d) = \Phi_2(x_d), \qquad d\Phi_1(x_d)/dx = d\Phi_2(x_d)/dx, \tag{45c, d}$$

$$d^2\Phi_1(x_d)/dx^2 = d^2\Phi_2(x_d)/dx^2, \qquad d^3\Phi_1(x_d)/dx^3 = d^3\Phi_2(x_d)/dx^3, \tag{45e, f}$$

$$\Phi_2(1) = 0, \qquad d^2\Phi_2(1)/dx^2 = 0. \tag{45g, h}$$

The eigenvalues for the segments are

$$\beta_1 = \alpha_1^4\gamma^2 - c_d\gamma, \qquad \text{and} \qquad \beta_2 = \alpha_2^4\gamma^2 - c_d\gamma. \tag{46a, b}$$

Because $\beta_1$ and $\beta_2$ are different, the eigenvalues and their higher powers can not be eliminated on a row by row basis, which increases the complexity of $[\Psi]$ and $[\Psi]'$.

Non-proportionality is introduced by systematically varying the ratio $\alpha_2^4/\alpha_1^4$ from unity. Given the definition of $\alpha^4$, a change in the ratio corresponds to a same sense change in the effective inertia or an opposite change in the effective stiffness of segment 2. Starting values for the solution are selected by noting that the frequency equation for a simply supported beam is

$$\sin(\beta) = 0, \tag{47}$$

which has roots at

$$\beta_n = n\pi, \qquad n = 1, 2, \ldots. \tag{48}$$

These values are used as estimates for the system undamped natural frequencies; damping ratios are determined from the equivalent proportionally damped solution. Both $\alpha^4$ values are initially taken as 3·0, the section discontinuity is located at $x_d = 0{\cdot}63$, and the damping coefficient is fixed at 25·0.

6.2.2. *Results and discussion*

The first two normalized eigenfunctions for an $\alpha^4$ ratio of 1·0 are shown in Figure 14. As expected, they indicate proportional damping, and display the classical displacement patterns and identically zero phase angles which are characteristic of such modes. When $\alpha_2^4$ is increased to 4·3 (see Figure 15), indications of non-proportionality begin to appear, especially in the second mode. Here the same magnitude discontinuities and phase shifts seen in example case 1 appear near the one undamped nodal point. In Figure 16(b), one can see that the instantaneous displacement magnitudes near the node are non-zero, and that the decreased effective stiffness of beam segment 2 results in smaller-displacement amplitudes for this portion of the beam.

The first mode exhibits few signs of non-proportionality. Inspection of Figure 16(a) indicates slightly smaller instantaneous modal displacements for segment 2, and numerical values of the phase angle deviate somewhat from zero, but a proportional damping

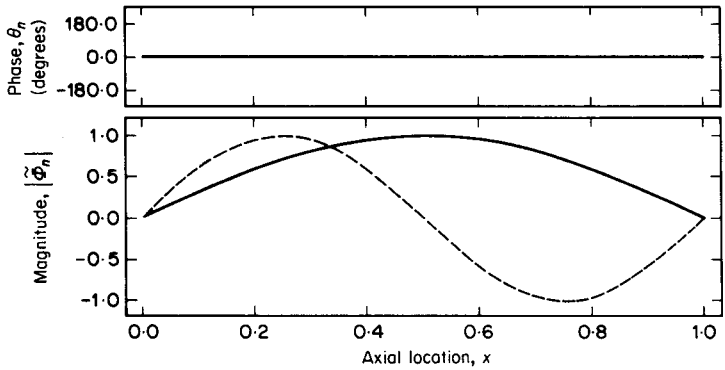


Figure 14. Normalized magnitude and phase for example case 2 eigenfunctions, $c_d = 25{\cdot}0$, $x_d = 0{\cdot}63$, $\alpha_2^4/\alpha_1^4 = 1{\cdot}0$. ——, Mode 1 ($\gamma_1 = -4{\cdot}167 \pm 3{\cdot}447i$); - - -, mode 2 ($\gamma_2 = -4{\cdot}167 \pm 22{\cdot}41i$).

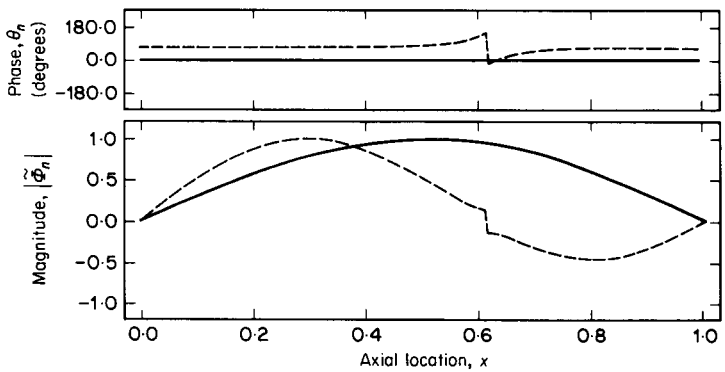


Figure 15. Normalized magnitude and phase for example case 2 eigenfunctions, $c_d = 25{\cdot}0$, $x_d = 0{\cdot}63$, $\alpha_2^4/\alpha_1^4 = 4{\cdot}3$. ——, Mode 1 ($\gamma_1 = -2{\cdot}322 \pm 3{\cdot}622i$); - - -, mode 2 ($\gamma_2 = -2{\cdot}969 \pm 16{\cdot}44i$).

assumption would undoubtedly be sufficient for this mode. This difference in behavior between the two modes is a function of the location of the second mode's undamped node relative to the source of the non-proportionalities. In this case the point tends to isolate part of system from the overall damping effect and thereby increase the effective non-proportionality. Note that the rapid decay in the mode 1 instantaneous displacements is characteristic of a proportionally damped system with a large damping ratio.

The solution algorithm performs well, with convergence occurring within 3–5 iterations for case 1, and 5–25 iterations for case 2. The differences are due to the larger damping coefficients and more complicated constraint matrix of the second system. For both cases, the highly non-proportional modes require the most computational effort. Experience has shown that the algorithm is quite tolerant of inaccurate starting values and large damping increments.

## 7. CONCLUDING REMARKS

The eigenproblem formulation and solution techniques discussed in the preceding pages allow determination of the complex natural frequencies and normal modes of transversely vibrating beams having a wide variety of non-proportional viscous damping configurations. These results are exact in that no simplifying assumptions are made regarding the eigensolution. The fact that a numerical solution procedure is used to solve

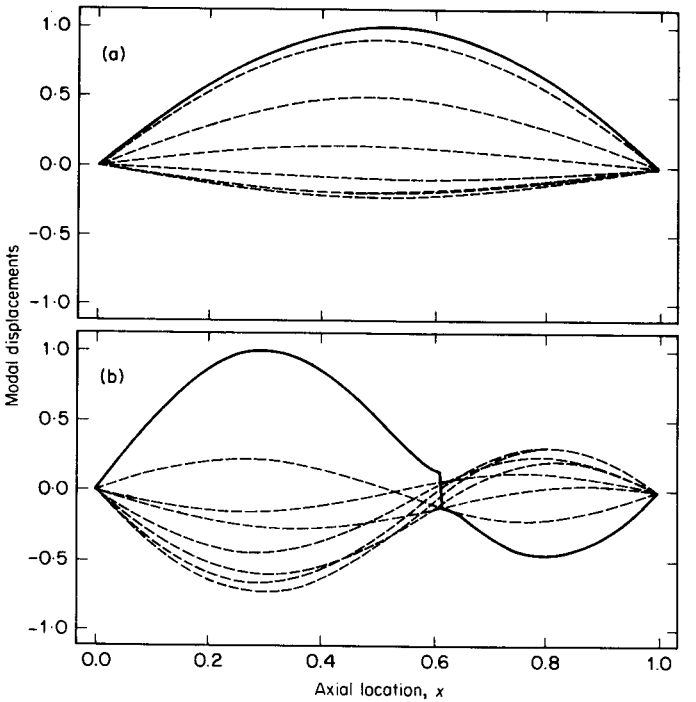


Figure 16. Time dependent modal displacements associated with example case 2 complex eigenfunctions, $c_d = 25{\cdot}0$, $x_d = 25{\cdot}0$, $\alpha_2^4/\alpha_1^4 = 4{\cdot}3$. (a) Mode 1, (b) mode 2. ——, Normalized magnitude; - - - -, instantaneous modal displacement.

the complex frequency equation is no more limiting than the numerical procedures used to solved the real frequency equation associated with classical cantilever beams. Our approach appears to be computationally efficient, and can easily be applied to cases in which non-proportionalities are created by arbitrary lumped or distributed impedances.

The suggested normalization techniques present complex domain modes in a manner which is complete, yet simple to interpret. Inspection of the resulting plots allows assessment of the locations and magnitudes of the system non-proportionalities. Interpretation is further improved when the magnitude-phase plots are supplemented with instantaneous modal displacement curves. The formulation/solution algorithm and normalization procedures can both be applied to other distributed parameter systems, including longitudinal rods, shafts, plates and shells. In addition, the normalization procedures can be used with lumped parameter systems, although care must be used during discretization to insure adequate spatial resolution near nodes, and with experimentally obtained data.

## REFERENCES

1. K. FOSS 1958 *Journal of Applied Mechanics* **25**, 361–364. Co-ordinates which uncouple the equations of motion of damped linear dynamic systems.
2. A. AL-JUMAILY and L. FAULKNER 1977 *Journal of Sound and Vibration* **54**, 203–213. Vibration of continuous systems with compliant boundaries.
3. L. BERGMAN and J. NICHOLSON 1985 *American Society of Mechanical Engineers Journal of Vibration, Acoustics, Stress, and Reliability in Design* **107**, 275–281. Forced vibration of a damped combined linear system.

4. R. SINGH and W. LYONS 1989 *American Society of Mechanical Engineers Noise and Vibrations Conference.* Complex eigenvalue solution of a longitudinal bar, fixed at one end and with a lumped damper at the other end.
5. J. ZAREK and B. GIBBS 1985 *Journal of Sound and Vibration* **78**, 185–196. The derivation of eigenvalues and mode shapes for the bending motion of a damped beam with general end conditions.
6. K. STEVENS, M. MARTINEZ and W. KELLY 1988 *SEM Sixth International Modal Analysis Conference Proceedings*, 1602–1608. A comparison of exact and approximate methods of analysis for added viscoelastic damping treatments.
7. K. STEVENS and S. SHOMSTEIN 1988 *SEM Sixth International Modal Analysis Conference Proceedings*, 1616–1622. Influence of partial viscoelastic damping treatments on the modal parameters of circular plates.
8. G. PRATER and R. SINGH 1986 *Journal of Sound and Vibration* **104**, 109–125. Quantification of the extent of non-proportional viscous damping in discrete vibratory systems.